ESTIMATING TREE CANOPY HEIGHT IN DENSELY FOREST-COVERED MOUNTAINOUS AREAS USING GEDI SPACEBORNE FULL-WAVEFORM DATA

Chun Liu[1], Shufan Wang[1,*]

[1]College of Surveying and Geo-informatics, Tongji University, Shanghai 200092, China
liuchun@tongji.edu.cn, W_shufan@tongji.edu.cn

Commission I, WG I/2

KEY WORDS: Tree canopy height, High vegetation coverage, Mountainous areas, GEDI, Waveform decomposition, Canopy height model.

ABSTRACT:

Tree canopy height is an important parameter for estimating forest carbon stock, and mountainous areas with dense vegetation cover are the main distribution areas of trees, so it is important to accurately measure the forest canopy height in mountainous areas with high vegetation cover. This paper focuses on the problem of poor inversion accuracy of canopy height estimation in large scale densely forest-covered mountainous areas, uses the complex echoes of GEDI full-waveform spaceborne laser in mountainous forests as the data source, improves the accuracy of forest canopy height estimation from multiple perspectives by improving the detection capability of weak and overlapping waves and constructing a canopy height model considering slope correction and environmental features. The results show that the modified RGD algorithm proposed in this paper can effectively detect the weak and overlapping waves in the echoes and improve the DTM/DSM inversion accuracy significantly (FVC>90%, R^2=0.8663/R^2=0.8073). In addition, the forest canopy height model is constructed on the basis of the physical geometric model of mountain slope and spatial environment characteristics, and finally the canopy height inversion accuracy of this paper is higher (FVC>90%, R^2=0.6729). The experiment proves that the model constructed in this paper is not only applicable to densely forest-covered mountainous areas, but also improves the accuracy of forest canopy height inversion in other environments. This study can provide technical and decision support for forest resource survey and global carbon balance.

1. INTRODUCTION

Forest ecosystems account for more than 80% of the global terrestrial carbon pool (Dixon et al., 1994) and play an important role in maintaining global carbon balance (Fang et al., 2001; Schimel et al., 2001). Mountain forests account for more than a quarter of the global forest, covering more than 9 million square kilometers of the earth's surface. In many countries, mountain forests are even the main form of tree existence. Take China as an example, more than 90% of the forests are distributed in mountainous areas. Therefore, rapid and accurate measurement of carbon stock in mountain forests has become an essential scientific demand (Seto et al., 2012). Meanwhile, canopy height is an important vertical structure parameter of forest ecosystem and a significant input feature for estimating forest biomass (Jin et al., 2018; Ni et al., 2015). Therefore, the accurate calculation of tree canopy height characteristics is a prerequisite for estimating mountain forest carbon stock, and how to improve the accuracy of canopy height estimation in densely forested mountain areas has become an urgent problem to be solved (Su et al., 2017).

Traditionally, forest canopy height monitoring is carried out by manual field measurements of randomly sampled plots. This method can only obtain data at the meter scale at a time, and is limited in mountainous forests with complex terrain. The emergence of remote sensing technology has solved this problem to a certain extent, and the wide coverage of remote sensing data has improved the efficiency of surface observation. Nowadays, optical images and radar have been used to estimate forest canopy height in some areas(BALZTER et al., 2007; Prush and Lohman, 2014; Zhang et al., 2014). However, in the dense montane forest, optical images and radar signals are limited by spectral saturation effect (Donoghue and Watt, 2006). These measurement methods cannot penetrate the forest canopy, lack direct probing of the vertical structure of vegetation, and lead to large errors in canopy height measurement (Keller, 2007; Lefsky et al., 2002). The emergence of LiDAR provides an alternative method for measuring forest canopy height, which can directly measure the three-dimensional structure of the forest and be not limited by saturation effects (Su et al., 2017).It is increasingly becoming an important tool for forest monitoring.

Spaceborne laser altimeter technology is to carry laser altimeter on satellites and other devices to obtain a broader range of earth observation data, accelerating the promotion of forest height mapping from the regional scale to the global scale(Jin et al., 2018). The Global Ecosystem Dynamics Investigation (GEDI) uses a full-waveform sampling system to sample light spots on the land surface to investigate the earth's ecosystems, providing the earth's highest resolution and most intensive spaceborne laser observations. However, in densely forest-covered mountainous areas, due to the influence of staggered leaves and terrain, the echoes not only contains weak and overlapping waveforms, but also are widened, which poses challenges to the forest height inversion algorithm.

Many scholars have realized the importance of complex waveform decomposition. Wagner found that a simple Gaussian decomposition model is hard to detect complex echoes accurately (Wagner et al., 2006). Chauve introduced the lognormal and generalized Gaussian function to explain the asymmetric waveform, but in most cases, the pulse waveform is still symmetrical (Chauve et al., 2008). Zhu proposed a method of progressive waveform decomposition, which extracted the waveforms of detected peaks one by one. However, the detection

---

* Corresponding author

accuracy of this method is not high for superimposed waveforms with only one prominent peak (Zhu et al., 2012). Lin proposed a method of rigorous Gaussian detection (RGD), which improved waveform recognition ability through the second derivative, but it has the problem of identifying waveform crests displacement (Lin et al., 2010). Current solutions to the problem of waveform spreading due to terrain generally fall into two categories: 1) Constructing a physical geometric model of slope. Quantifying the effect of terrain on forest canopy height estimation by constructing model equations (Allouis et al., 2012; Lee et al., 2011). This method has a wide range of application and simple principle, but there are still some errors in the area with large topographic fluctuations. 2) Build a regression model of vegetation structure parameters. Extract waveform parameters from the echoes and build a regression model between these parameters and canopy height, thus indirectly attenuating the effect of spreading(Lefsky et al., 2005; Lefsky, 2010). This type of method can achieve relatively good accuracy, but the inversion results are affected by the accuracy of waveform parameter extraction. In summary, the current studies all focus on a single problem in the height inversion of mountain forests, and lack a multi-faceted approach to consider the overall improvement of canopy height inversion accuracy of montane forests.

Therefore, this study addresses the problem of poor accuracy of maximum canopy height inversion of dense mountain forests by full-waveform satellite-based laser. The densely forest-covered mountainous area is taken as the main research object. For the definition of dense forest, the fractional vegetation coverage (FVC) is calculated from the multi-spectral images in this paper, and the area with vegetation cover greater than 70 % is defined as the dense forest-covered area (Tsutsumida et al., 2019; Li et al., 2021; Wei et al., 2018). FVC is defined as the ratio of green vegetation vertical projected area to the considered land surface extension, is a crucial biophysical property of vegetation and an important parameter that can quantify the vegetation horizontal structure. At present, the common way of calculating FVC is indirect calculation through NDVI. The calculation formula is as follows:

$$f_c = \frac{NDVI - NDVI_s}{NDVI_v - NDVI_s} \qquad (1)$$

where f_c is FVC ; $NDVI$ is a weighted average of vegetation and non-vegetation regions; $NDVI_s$ is the vegetation index of the bare soil pixels; and $NDVI_v$ is the vegetation index of the whole vegetation cover.

In this paper, we propose a method for modeling the maximum canopy height of forest that integrates the ability to enhance waveform decomposition and slope correction. For the complex echoes of montane areas, firstly, the echoes including weak and overlapping waves are accurately identified through an modified RGD algorithm to extract the three-dimensional structural features of forest. Then, a canopy height regression model considering the slope geometry principle, vertical structure of trees and spatial environment features of the forest is constructed. The method proposed in this paper not only improves the ability to extract forest features in full-waveform complex echoes, but also integrates topographic and spatial element information to improve the accuracy of overall canopy height inversion. The main contributions of this paper are as follows：

1) A modified RGD algorithm is proposed to detect weak and overlapping waves in waveforms by detecting peaks and inflection points, and to improve the decomposition accuracy of full waveforms in complex dense mountain forest echoes.
2) A slope-correction-based maximum canopy height modeling method is constructed to provide a more accurate inversion of

mountain forest canopy height by integrating the physical geometric model of mountain slope and the vertical structure of vegetation with spatial environmental characteristics.
3) Evaluate the performance of the modified RGD algorithm proposed in this paper, compare and analyze the accuracy with the official GEDI algorithm.
4) Compare and analyze the final inversion results of this paper with the regional airborne laser scanning (ALS) acquisition height.

2. METHODOLOGY

The proposed method mainly consists of two parts: 1) A modified RGD waveform decomposition algorithm. To improve the detection ability of weak and overlapping pluses in complex echoes of mountain forests, and extract the three-dimensional structure characteristics of trees. 2) Forest canopy height model with slope correction. A forest canopy height inversion model is constructed considering the geometric principle of mountain slope, vertical structure of vegetation and characteristics of forest spatial environment.

2.1 A Modified RGD Waveform Decomposition Algorithm

According to Wagner's theory(Wagner et al., 2006), the shape of the transmitted waveforms is a Gaussian-like distribution. The received echoes signal are the sum of all target echoes passing through in transmitting the pulses to the ground, so it can be regarded as a superposition of multiple Gaussian models. The Gaussian target can be expressed by the following formula, considering the background noise:

$$P_r(x) = \sum_{i=1}^{N} \varphi_i(x) + b \qquad (2)$$

$$\varphi_i(x) = A_i \cdot \exp\left[-\frac{(x - \mu_i)^2}{2\delta_i^2}\right] \qquad (3)$$

Where $\varphi_i(x)$ is the ith component of the Gaussian function, b is the noise offset estimation, A_i is the amplitude of the ith Gaussian, μ_i is the coordinate position corresponding to the ith Gaussian peak, σ_i is the standard deviation of the ith Gaussian, N is the number of Gaussians.

In the high-vegetation-covered region, due to overlapping vegetation leaves, target echoes exist in the form of weak and overlapping pluses in addition to apparent peaks. Ignoring such waveforms will affect the elevation accuracy of inversion. Therefore, to improve the recognition accuracy of weak and overlapping pluses, the modified RGD algorithm is proposed in this study:

1) Gaussian filtering. Firstly, as described in the GEDI Algorithm Theoretical Basis Document (ATBD), the full waveform smoothing is performed with Gaussian filter of width 6.5ns based on the transmit waveform parameters. The first and last positions in the waveform where the signal intensity is above the following thresholds are identified as *searchstart* and *searchend*, respectively:

$$\text{threshold} = \text{mean} + \sigma \cdot \upsilon \qquad (4)$$

where mean is the mean noise level, σ is the standard deviation of noise of the smoothed waveform, and υ is a constant currently set at 4.
2) Peak detection of adaptive thresholds. The maximum amplitude value of the 20samples before and after the waveform is used as the noise threshold. The highest and lowest locations

in the range between *searchstart* and *searchend* are searched for as *toploc* and *botloc*, respectively, and the range between them is the subsequent waveform processing range. The local maximum peak method is used to find the echo location that is higher than the noise threshold. The number of peaks found is recorded as M.

3) Waveform decomposition combining the peak and the second derivative. The second derivative of the waveform is calculated, and the zero value is marked as the inflection point. When the number of inflection points is 2M, a pulse is determined by a peak point and the two closest inflection points to the peak. The half-waveform width (FWHM), an important parameter in Gaussian fitting, is two times the distance between the peak and the nearest inflection point (Figure 2(a)(b)). When the number of inflection points is greater than 2M, the extra inflection points represent hidden waveform peaks (Figure 2(c)). Firstly, for the detected waveform peaks, the parameters are determined by using the same method as before, and the waveform of the determined parameters is stripped until M=0 (Figure 2(d)). In the remaining inflection points, the point with the larger amplitude is taken as the hidden waveform peak, and the nearest inflection point is taken as its inflection point, half-waveform width is obtained by calculating twice the distance between the crest and the inflection point (Figure 2(e)). After the parameters are determined, the waveform is stripped and iterated repeatedly until the decomposition is completed.

In this paper, the relationship between different types of weak and superimposed waves and peaks and inflection points are simulated, as shown in Figure 1. It can be seen from Figure 1 that the modified algorithm in this paper can not only detect the hidden waveform but also reduce the redundancy of peak detection and be more accurate in extracting the location of the hidden waveforms compared with the original RGD algorithm.
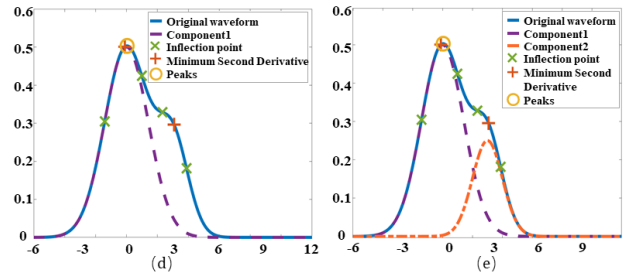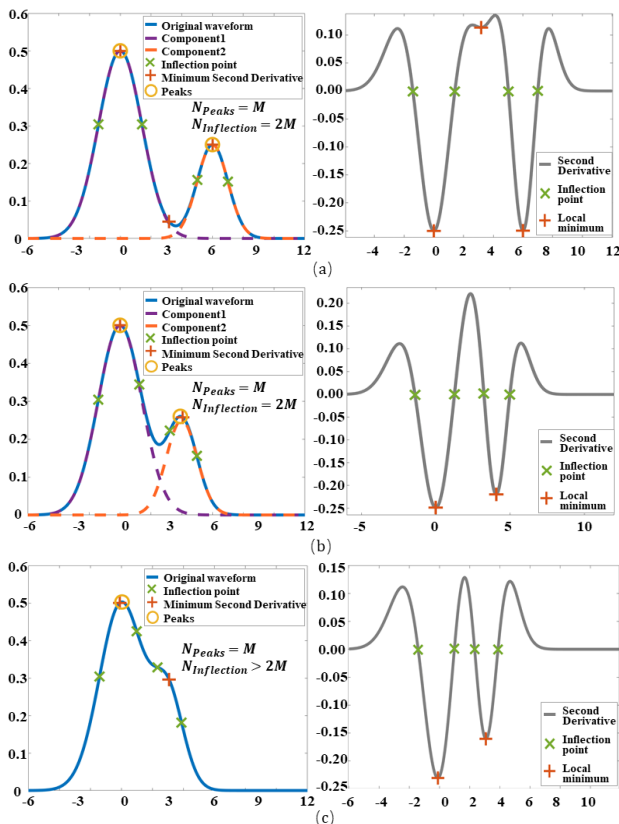

(a)

(b)

(c)

(d)

(e)

Figure 1. Simulate the superposition relationship between two received waveforms returned with different separations and amplitudes: (a) the left figure shows the waveform superposition status (6ns separation) and waveform feature points. The right figure shows the second derivatives curve of the whole echo and the corresponding position of waveform characteristic points. (b) the left figure shows the waveforms' superposition status (4ns). (c) the left figure shows the waveforms' superposition status (2ns). (d) the waveform of the peak detected in the echo with pulses interval 2ns (e) the waveform of an inflection point as its peak in the echo with pulses interval 2ns.

2.2 Forest Canopy Height Model With Slope Correction

Height parameters commonly used in vegetation height inversion are extracted from the results of decomposition (Figure 2), and the meanings of these peremeters are shown in Table 1.

Parameter	Description
Toploc	Sample number of highest detected return
Botloc	Sample number of lowest detected return
CanopyPeak	The location of the first detected mode peak
GroundPeak	The location of the last detected mode peak
MaxPeak	The location of the maximum amplitude
Extent	The distance between Toploc and Botloc
PeakLeg	The distance between the first mode peak and last mode peak
CanopyLeg	The distance between TopLoc and the last detected mode peak

Table 1. Extracted waveform features.

The laser zenith Angle is approximated as $0°$. The impact of mountain slope on canopy height can be abstracted into a physical model shown in Figure 2(b). The tangent function can be used to calculate the maximum slope height caused by terrain. However, it can also be seen from Figure 2(b) that even trees in the same footprint are affected by different slope heights due to their different positions. As the location of the tree rises, it is more affected by the slope height. Therefore, position coefficient α is introduced in this paper. The height correction model of slope-shaped vegetation adopted in this paper is as follows:

$$H_m = H_{Extent} - \alpha \times D \times \tan(\theta) + \varepsilon \qquad (5)$$

Where H_m represents the corrected vegetation height, H_{Extent} represents the waveform length, α represents the position coefficient, D represents the footprint diameter, θ represents the terrain slope in degrees (°), and ε represents the correction constant.

When GEDI is used as the laser data source, D=25 m. The values of α position coefficient and ε correction constant in the vegetation slope physical model are determined by linear regression algorithm, and the results of maximum canopy height after physical correction of slope are obtained by substituting the waveform length and topographic slope within the 3×3 neighborhood window.
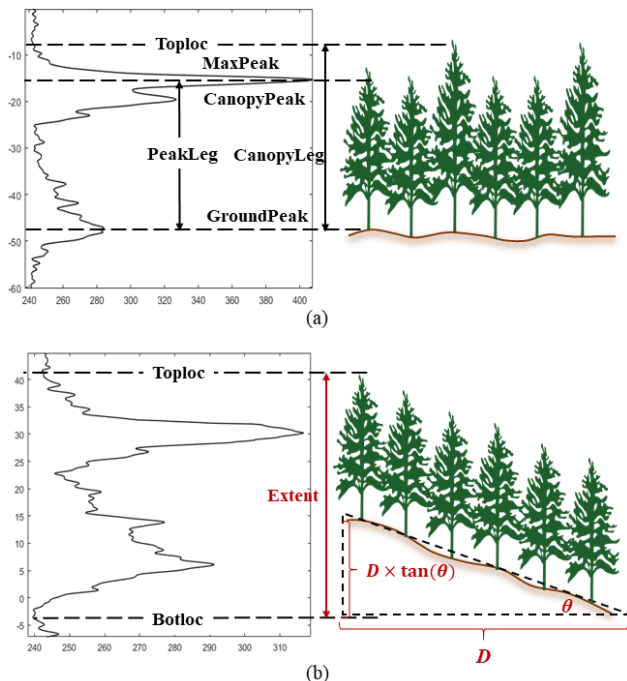

(a)

(b)

Figure 2. Physical models of vegetation slope

However, in densely forest-covered mountainous areas, the accuracy of vegetation height estimation is affected not only by the topographic slope, but also by the structure of the vegetation and the spatial environment. Therefore we consider multiple features and analyze the feature importance by random forest and multiple linear regression methods. The feature meanings are shown in Table2, and Fig3 shows the top 5 feature parameters ranked with the importance of forest canopy height. A model for vegetation height estimation in densely forest-covered mountainous areas is developed by polynomial stepwise nonlinear regression algorithm as follows:

$$H_{CHM} = f(MeanFVC, H_m, Latitude, MaxPeak) \quad (6)$$

Where H_{CHM} represents estimated vegetation height, *MeanFVC* represents the average FVC and *Latitude* represents the footprint Latitude.
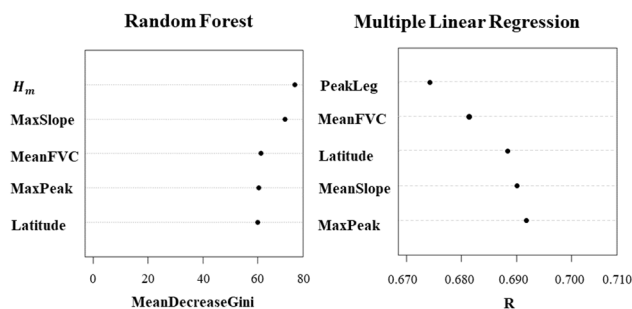

Figure 3. Order of characteristic importance

Parameter	Description
MaxSlope/MeanSlope	Max/Mean slope
MaxFVC/MeanFVC	Max/Mean FVC
Latitude	Latitude of footprint
Longitude	Longitude of footprint

Table 2. Vegetation and spatial environmental features.

3. EXPERIMENT AND RESULTS

3.1 Experiment Area and Data

The experimental area is located on the east bank of Chesapeake Bay, Maryland, USA. It is about 10km*10km in size(Figure 4). which is a typical mountainous forest area. The vegetation type of the study area is deciduous broad-leaved forest, and the average canopy height is about 38m. The vegetation coverage here is high, the percentage of vegetation coverage in most areas is more than 70 percent. In addition, the area is highly undulating, with an altitude of 0~43m and a mountain slope of 0~45°. Therefore, the experimental area is a representative area of densely forest-covered mountainous areas.
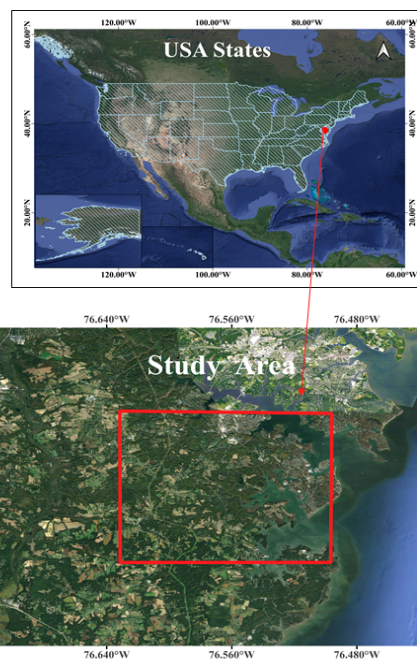

Figure 4. Study area location.

GEDI is used as an spaceborne full-waveform data source. GEDI acquires waveforms over eight tracks of data, illuminating the ground at a frequency of 242Hz over a diameter of 25m, which is known as the footprint. The footprints on the same track are separated by 60 m, and the track-to-track distance is 600 m. We use GEDI L1B and L2A level data for this study. The multispectral data were obtained using high-resolution Sentinel-2 satellite data. The Band2 (B), Band3 (G), Band4 (R), and Band8 (NIR) bands of the L2A-level data are fused to generate multispectral image data with 10m spatial resolution. In this paper, airborne laser point cloud and derived DTM\DSM\CHM data are used as validation data for the study area, and the airborne data were collected in August 2021 using Teledyne Optech Galaxy Prime with an average point cloud density of 35.41 pts/m^2. The flight campaign was conducted by the

National Ecological Observatory Network (NEON) Airborne Observation Platform(National, 2021).

3.2 Waveform Decomposition Results

We compared the waveform decomposition results of our algorithm with the results of the decomposition algorithm proposed by Jin, which was adopted as GEDI official decomposition algorithm (Hofton et al., 2000a; Hofton et al., 2000b). Figure 5 shows the difference in the decomposition of the two algorithms in the actual echoes. From (a)(b), it can be seen that there is an overlapping wave to the left of the main peak, but the official algorithm only detects one pulse of the main peak, while the algorithm of ours identifies the overlapping weak wave better and reduces the DTM error from 6.25m to 0.77m; (c)(d), the original waveform consists of multiple weak and overlapping waves at close distances, and again, while the official algorithm only detects one peak, our algorithm decomposes a total of four waveforms, reducing the DTM error from 28.15m to only -0.08m and the DSM error to -0.18m.

However, at the same time, the DSM error in (a)(b) increases slightly, which we analyze due to the peak displacement monitored as a result of filtering.
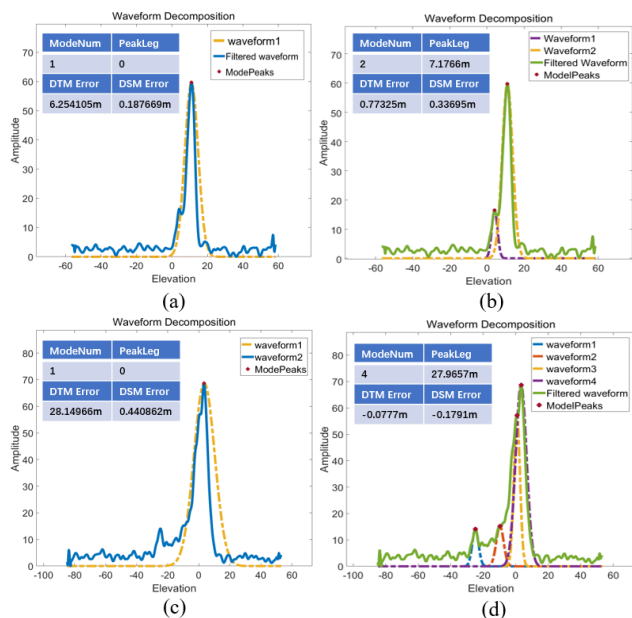

Figure 5. Comparison of waveform decomposition results

We evaluated the agreement between vegetation height inversion accuracy and ALS observations using four statistical metrics: bias, coefficient of determination (R^2), root-mean-square error ($RMSE$) and root-mean-square-percentage error ($RMSPE$).
The results in Fig. 6 show the fitting degree of ours and the official decomposition algorithm to DTM and DSM under different FVC (90~100%, 80~90%). In the inversion of DTM, our the algorithm improved the R^2 accuracy to 0.8663 and 0.9172 for 90~100% and 80~90%, respectively; relatively speaking, the inversion of DSM achieved a greater improvement, improving the R^2 accuracy from 0.5150 and 0.6409 to 0.8073 and 0.8291 for 90~100% and 80~90%, respectively.

In the algorithm of left figures, the weak detection of overlapping waveforms makes the lowest position waveform obtained from the decomposition higher than the ground and the highest position waveform lower than the canopy. The modified RGD

algorithm proposed in this paper improves the detection of weak and overlapping waves by combining peak detection with second-order derivatives, therefore, the accuracy of the fit to DTM and DSM has been greatly improved.
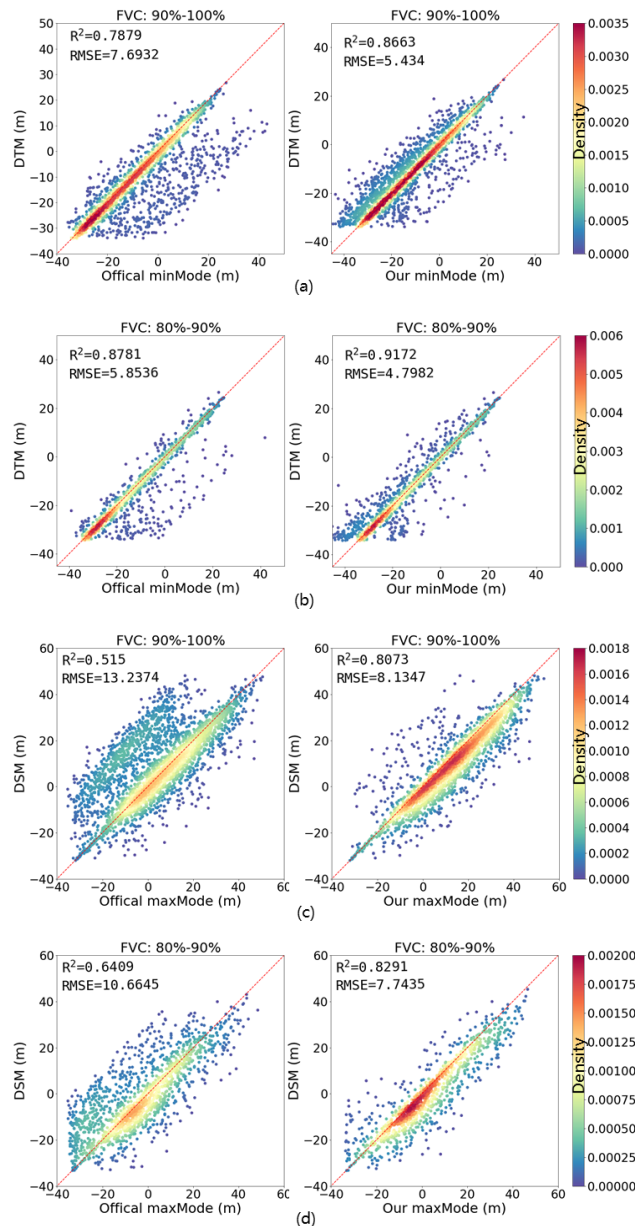

Figure 6. Comparison of decomposition accuracy between our modified algorithm and the official algorithm: (a) comparison of inversion accuracy of DTM in the region of FVC>90% (b) comparison of inversion accuracy of DTM in the region of FVC>80% (c) comparison of inversion accuracy of DSM in the region of FVC>90% (d) comparison of inversion accuracy of DSM in the region of FVC>80%

3.3 Forest Canopy Height Inversion Results

In Fig. 7 we compare the fitting degree to the maximum forest canopy height at different FVCs. In the region of FVC>90%, the feature $maxmode-minmode$ of official algorithm does not fit well with the ALS collected canopy height values, with R^2 only 0.369 and $RMSE$ of 15.6774. The modified RGD decomposition algorithm improves R^2 to 0.5098 and $RMSE$ to 7.3447. After the canopy height modelling, there is a further

improvement , R^2 reaches 0.6729 and $RMSE$ decreases to 5.7944. In the region of FVC>80%, the R^2 and $RMSE$ are improved from the original 0.2164, 12.1577 to 0.4984 and 9.2268 by the modified waveform decomposition algorithm, and then to 0.6940 and 5.5961 by modeling.

This is because the model in this paper can better solve the waveform broadening caused by terrain, model tree height based on position and waveform characteristics, and comprehensively consider the environment and waveform characteristics, so that the fitting accuracy of tree height can be better.

However, it can also be seen in Figure 7 that although our decomposition algorithm can improve the detection of overlapping waves to a certain extent, there is still a situation that the PeakLeg of some waveforms is calculated as 0. This may be due to the fact that in a dense forest, the distance between reflected pulses is too close causing the two pulses to be spaced less than one bin apart in the received echoes, which can only be shown as one waveform. Under such data conditions, the processing effect of the method in this paper is limited.
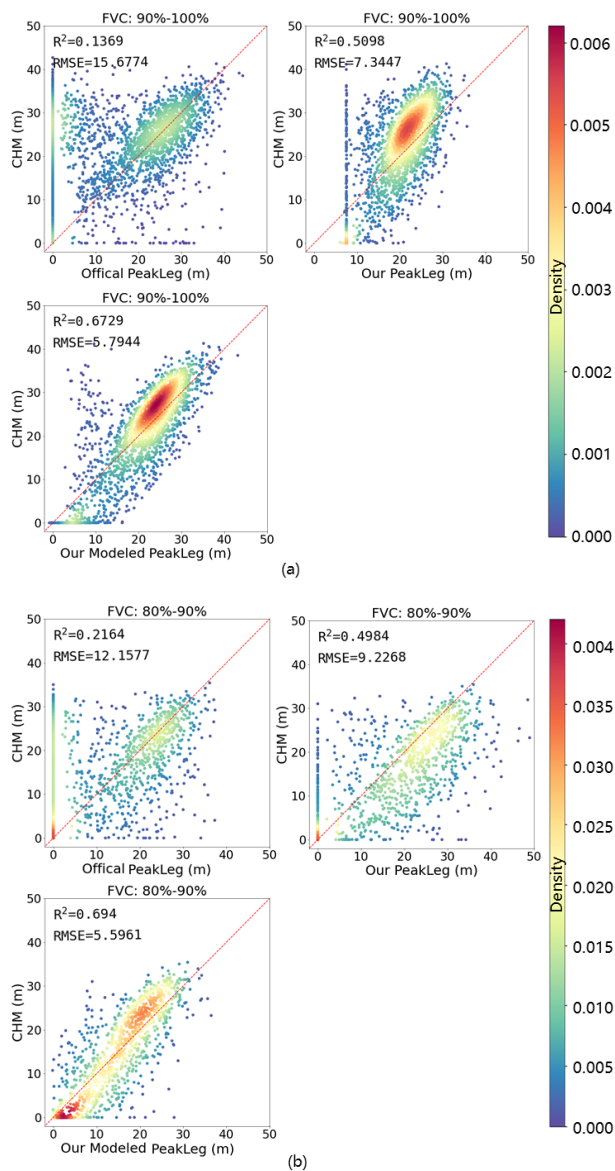

Figure 7. Comparison of the accuracy of our forest canopy height modeling results with the official algorithm: (a) Comparison of

forest canopy height inversion accuracy in the region with FVC>90%, top left is the official algorithm result, top right is the result of our modified decomposition algorithm, bottom left is our final forest height model inversion result (b) Comparison of forest canopy height inversion accuracy in the region with FVC>80%

Finally, we selected several typical mountain echoes with different FVC for canopy height extraction and verification (Figure 8), the FVC of (a), (b) and (c) decreased successively. It can be seen from Figure 8 that although RMSPE can be reduced to less than 12% only by our waveform decomposition algorithm, it was still significantly higher in high FVC areas than in low FVC areas. After combining the forest canopy height model, RMSPE in high FVC areas decreased significantly.And in the low FVC area, although the waveform decomposition is enough to RMSPE has reached 1.80%, the RMSPE of the canopy height model output is even lower, reaching 1.19%, indicating that the canopy height model constructed in this paper for the high vegetation cover mountain area also has good effect in the low vegetation cover area.

4. DISCUSSION AND CONCLUSIONS

To deal with the problem of poor inversion accuracy of space-borne full-waveform data for tree heights in densely forest-covered mountainous areas, this paper proposes a tree height inversion method that integrates waveform decomposition capacity enhancement with canopy height modeling based on slope correction. The two main contributions of this method are 1) proposing an modified rigorous pulse detection algorithm to improve the detection of complex overlapping and weak waves and extract more accurate vertical structure features of vegetation, and 2) constructing a tree height estimation model that considers the influence of slope and environmental factors to attenuate the lack of accuracy caused by dense vegetation and topographic slope.

To demonstrate our method, we compared the accuracy with the official algorithm. Qualitative and quantitative validation shows that the features proposed by our modified RGD algorithm have a substantial improvement in the fitting of DTM\DSM\CHM. And the canopy height model constructed in this paper makes the accuracy of tree height fitting further improved. This shows the necessity of considering the topographic and spatial environment features comprehensively. The experiments also demonstrate that the tree height inversion model in this paper is not only applicable to high vegetation cover mountain area, but also applicable in low vegetation cover areas.

Our method improves the accuracy of tree height inversion of spaceborne full-waveform lidar data in densely forest-covered mountainous areas. The research results can provide technical support for large-scale and efficient forest resource investigation, and then provide a decision-making basis for the measurement and realization of the global carbon balance. Based on this method, expanding spatial environment factors can improve the model's spatial adaptability, further broadening the scope of application. Furthermore, this method can provide a reference for large-scale and high-precision forest three-dimensional structure inversion.

Although the method proposed in this paper improves the accuracy of full-waveform laser inversion of forest canopy height in densely mountainous areas. When the received pulses have too small waveform distance resulting in only one wave peak being displayed between overlapping waves, the processing effect of

our method is limited under such data conditions. Therefore, future work can be devoted to data fusion approaches with the aim to overcome such limitations, which is also a direction of our future work.
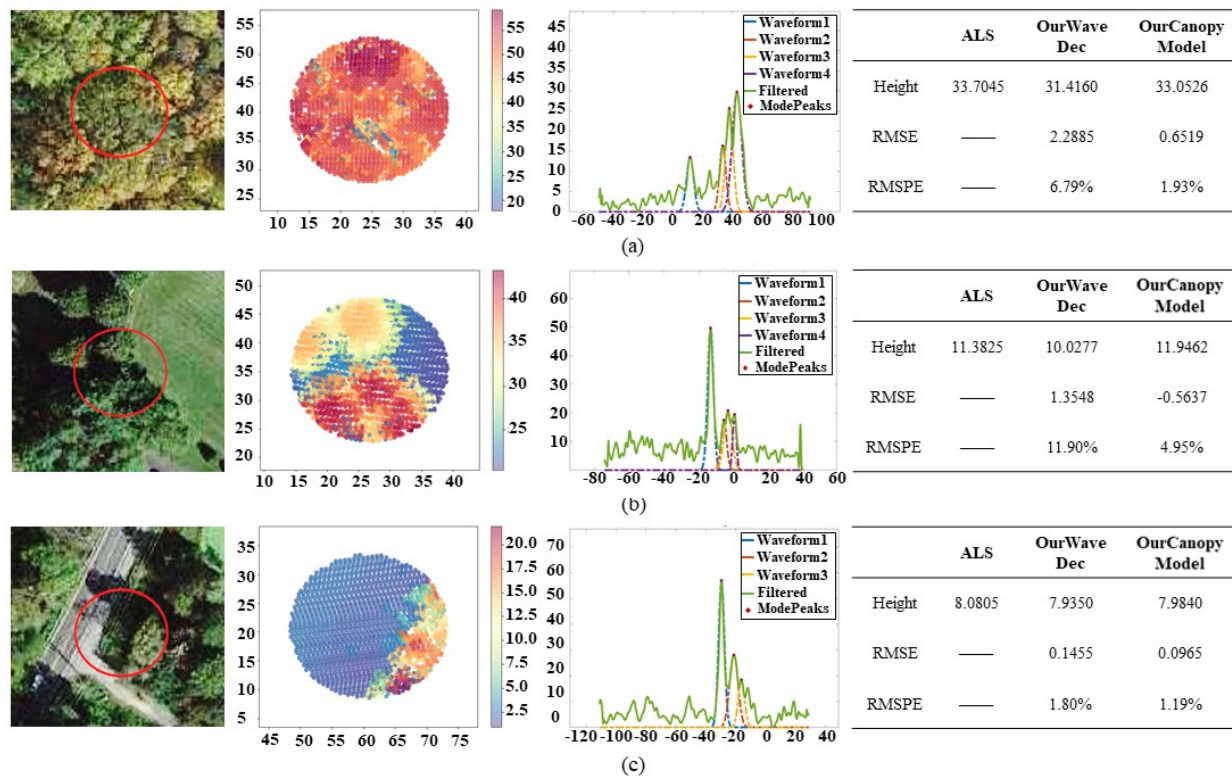

Figure8. Verification of canopy height inversion accuracy in typical forest-covered mountainous areas: (a)(b)(c) from left to right are remote sensing images, point cloud top view colored with height, waveform decomposition results and tree high precision comparison table. The tree high precision comparison table contains the comparison of airborne laser inversion tree height, waveform decomposition algorithm results and tree height modeling results in this paper.

REFERENCES

Allouis, T., Durrieu, S. and Couteron, P., 2012. A New Method for Incorporating Hillslope Effects to Improve Canopy-Height Estimates From Large-Footprint LIDAR Waveforms. *IEEE Geoscience and Remote Sensing Letters*, 9(4): 730-734.

BALZTER, H., ROWLAND, C. and SAICH, P., 2007. Forest canopy height and carbon estimation at Monks Wood National Nature Reserve, UK, using dual-wavelength SAR interferometry. *Remote Sensing of Environment*, 108(3): 224-239.

Chauve, A., Mallet, C., Bretar, F., Durrieu, S. and Deseilligny, M., 2008. Processing Full-Waveform Lidar Data: Modelling Raw Signals. *ISPRS Workshop on Laser Scanning 2007 and SilviLaser 2007*.

Dixon, R.K. et al., 1994b. Carbon Pools and Flux of Global Forest Ecosystems. *Science*, 263(5144): 185-190.

Donoghue, D.N.M. and Watt, P.J., 2006. Using LiDAR to compare forest height estimates from IKONOS and Landsat ETM+ data in Sitka spruce plantation forests. *International Journal of Remote Sensing*, 27(11): 2161-2175.

Fang, J., Chen, A., Peng, C., Zhao, S. and Ci, L., 2001. Changes in forest biomass carbon storage in China between 1949 and 1998. *Science*, 292(5525): 2320-2.

Hofton, M.A. et al., 2000. An airborne scanning laser altimetry survey of Long Valley, California. *International Journal of Remote Sensing*, 21(12): 2413-2437.

Hofton, M.A., Minster, J.B. and Blair, J.B., 2000. Decomposition of laser altimeter waveforms. *IEEE transactions on geoscience and remote sensing*, 38(4): 1989-1996.

Jin, S. et al., 2018a. The Transferability of Random Forest in Canopy Height Estimation from Multi-Source Remote Sensing Data. *Remote Sensing*, 10(8): 1183.

Keller, M., 2007. Revised method for forest canopy height estimation from Geoscience Laser Altimeter System waveforms. *Journal of Applied Remote Sensing*, 1(1): 013537.

Lee, S., Ni-Meister, W., Yang, W. and Chen, Q., 2011. Physically based vertical vegetation structure retrieval from ICESat data: Validation using LVIS in White Mountain National Forest, New Hampshire, USA. *Remote Sensing of Environment*, 115(11): 2776-2785.

Lefsky, M.A. et al., 2005. Estimates of forest canopy height and aboveground biomass using ICESat. *Geophysical Research Letters*, 330(5)

Lefsky, M.A., 2010. A global forest canopy height map from the Moderate Resolution Imaging Spectroradiometer and the Geoscience Laser Altimeter System. *Geophysical Research Letters*, 37(15)

Lefsky, M.A., Cohen, W.B., Parker, G.G. and Harding, D.J., 2002. Lidar Remote Sensing for Ecosystem Studies. *Bioscience*, 52(1): 19-30.

Li, M. et al., 2021. Fractional vegetation coverage downscaling inversion method based on Land Remote-Sensing Satellite (System, Landsat-8) and polarization decomposition of Radarsat-2. *International journal of remote sensing*, 42(9): 3255-3276.

Lin, Y., Mills, J.P. and Smith-Voysey, S., 2010. Rigorous pulse detection from full-waveform airborne laser scanning data. *International journal of remote sensing*, 31(5): 1303-1324.

National, E.O.N.N., 2021. Discrete return LiDAR point cloud (DP1.30003.001). National Ecological Observatory Network (NEON).

Ni, X. et al., 2015. Mapping Forest Canopy Height over Continental China Using Multi-Source Remote Sensing Data. *Remote Sensing*, 7(7): 8436-8452.

Prush, V. and Lohman, R., 2014. Forest Canopy Heights in the Pacific Northwest Based on InSAR Phase Discontinuities across Short Spatial Scales. *Remote Sensing*, 6(4): 3210-3226.

Schimel, D.S. et al., 2001. Recent patterns and mechanisms of carbon exchange by terrestrial ecosystems. *Nature*, 414(6860): 169-72.

Seto, K.C., Guneralp, B. and Hutyra, L.R., 2012. Global forecasts of urban expansion to 2030 and direct impacts on biodiversity and carbon pools. *Proceedings of the National Academy of Sciences*, 109(40): 16083-16088.

Su, Y., Ma, Q. and Guo, Q., 2017a. Fine-resolution forest tree height estimation across the Sierra Nevada through the integration of spaceborne LiDAR, airborne LiDAR, and optical imagery. *International journal of digital earth*, 10(3): 307-323.

Tsutsumida, N. et al., 2019b. Mapping spatial accuracy of forest type classification in jaxas high-resolution land use and land cover map. *ISPRS Annals of the Photogrammetry, Remote Sensing and Spatial Information Sciences*, IV-3/W1: 57-63.

Wagner, W., Ullrich, A., Ducic, V., Melzer, T. and Studnicka, N., 2006. Gaussian decomposition and calibration of a novel small-footprint full-waveform digitising airborne laser scanner. *ISPRS Journal of Photogrammetry and Remote Sensing*, 60(2): 100-112.

Wei, X., Wang, S. and Wang, Y., 2018. Spatial and temporal change of fractional vegetation cover in North-western China from 2000 to 2010. *Geological Journal*, 53: 427-434.

Zhang, G. et al., 2014. Estimation of forest aboveground biomass in California using canopy height and leaf area index estimated from satellite data. *Remote Sensing of Environment*, 151: 44-56.

Zhu, J., Zhang, Z., Hu, X. and Li, Z., 2012. Analysis and Application of LIDAR Waveform Data Using a Progressive Waveform Decomposition Method. *International archives of the photogrammetry, remote sensing and spatial information sciences.*, XXXVIII-5/W12: 31-36.